BACKGROUND

Modeling the diffusion process of water molecules in brain tissues is definitely a complicated task to perform in vivo, as it requires to deal with the hardware limitations of MRI systems as well as with the scan duration that cannot be greater than an hour with human volunteers or four to six ours with animals. Post-mortem studies can be a solution, but the diffusion process in known to be really altered as the metabolism is stopped (for instance, the average diffusion coefficient is divided by a factor of three), and because the fixation using paraformaldehyd strongly modifies the microstructure of the tissues building bridges between membranes.
Based on these considerations, we have decided in the frame of this proposal to develop a large-scale Monte-Carlo simulator dedicated to create numerical phantoms mimicking the structure of brain tissues that can be used to perform in silico experiments useful to infer, refine, and validate the modeling of the diffusion process of water molecules.

OBJECTIVES

Our first objective was to develop a numerical simulator of the diffusion process with the following characteristics:

1. the simulator should allow to create any configuration of membrane, should it be purely synthetic or stemming from the analysis of a real tissue
2. the simulator should allow to modify locally the diffusion model such that, for instance, the model can vary according to the distance to the membrane, or according the local metabolism
3. the simulator must be fast enough to create in silico diffusion processes in a reasonable time
4. the simulator should allow to simulate diffusion-weighted MR images stemming from any MRI pulse sequence (pulsed gradient spin echo, oscillating gradient spin echo, double pulsed gradient spin echo, arbitrary spin echo, ….)

Our second objective was to validate the simulator using simple membrane geometry and models, in order to check its efficacy and accuracy.

Our third objective was to use this simulator to investigate more fundamental questions of the community, for instance the effect of cell swelling of the apparent diffusion coefficient, or a better undertsanding of the diffusion process withing gray and white matter developing specific geometries mimicking the two tissue cellular environments.

SOFTWARE DEVELOPMENTS

We combined a Monte Carlo Brownian dynamics simulator capable of simulating diffusion of spins in arbitrarily complex geometries with a DW signal integrator emulating various MR pulse sequences. The flexibility and ability of Monte-Carlo modeling enabled us to investigate detail dynamics and mechanisms of molecular diffusion in complex systems which cannot be handled through analytical models. Hence, we have developed software to reproduce various tissue configurations using dynamic meshes. Complicated geometries mimicking neural tissue components, such as neurons, astrocytes, axons, etc. can be emulated, as well as tissue features (e.g. cell size, density, membrane permeability) and basic diffusion mechanisms in different compartments (presence of attractors, local viscosity, membrane interactions, etc.). This framework allowed to bridge the gap between elementary processes occurring at a micrometer scale and the resulting DW signal measured at millimeter scale, providing a better understanding of the features observed in DW MRI (variation of apparent diffusion coefficient (ADC) with cell size, diffusion anisotropy) and to optimize acquisition schemes for different applications (e.g. fiber-tracking algorithms).

The simulation code was implemented in C++ on a high computing PC cluster for large-scale simulations, and main features are described as following:

- Cell membranes are generated using meshes in order to model different cell types with heterogeneous shapes and sizes. This module allows users to specify cell properties including the thickness, permeability, and diffusion coefficient (D) inside and close to the membrane layers. In addition, we incorporated the mesh with dynamic morphological evolution, thus it can be utilized to simulate sequential changes of tissue shapes including expansion, shrinkage, and deformation.
- Diffusing particles ("spins") are modelled as random walkers which are initially randomly distributed in a three dimensional space. The average free displacement of each "spin" for an elementary time step of length dt is scaled to its associated compartmental D based on the Einstein equation, i.e. <x>=(6Ddt)1/2. For each simulation step, the spatial positions of particles are updated subject to a series of potential interactions: (i) In accordance with the permeability, the particle may penetrate through the related cell membrane or be elastically reflected. (ii) The diffusivity of the particle may be modified into that of the interacting membrane layers.
- The MR pulse sequence module is flexible to model a variety of pulse sequences with different combinations of radio frequency (RF) and gradient pulses. The gradient pulse is characterized using any shape (trapezoids, oscillating gradients, CHIRP, ...). Parameters including the magnitude (g), the rising and descending ramp times, the duration (δ) and separation (Δ) of the diffusion gradient pulses are adjustable

The next figures provides an overview of the design of the Diffusion Monte-Carlo Simulator (called BrainVISA/Microscopist) and a UML diagram of the source code, highlighting the complete separation between the Monte-Carlo part dedicated to the simulation of the movement of molecules in a geometry of membranes and the MR image synthesizer simulating the MRI system to deliver diffusion-weighted MRI data.

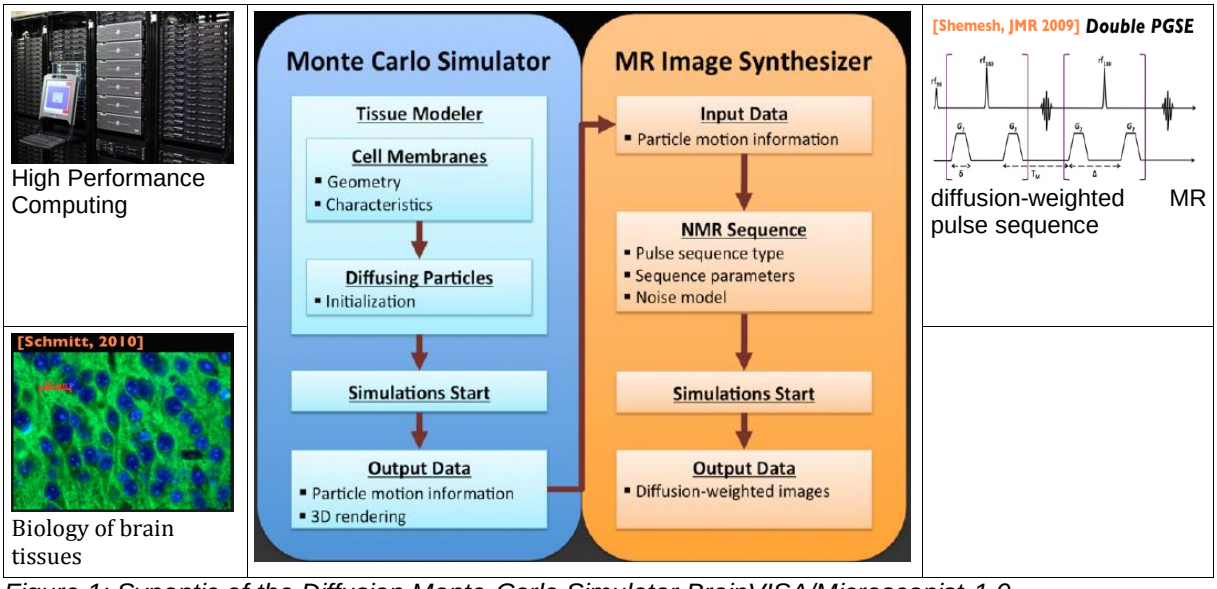

Figure 1: Synoptic of the Diffusion Monte-Carlo Simulator BrainVISA/Microscopist-1.0

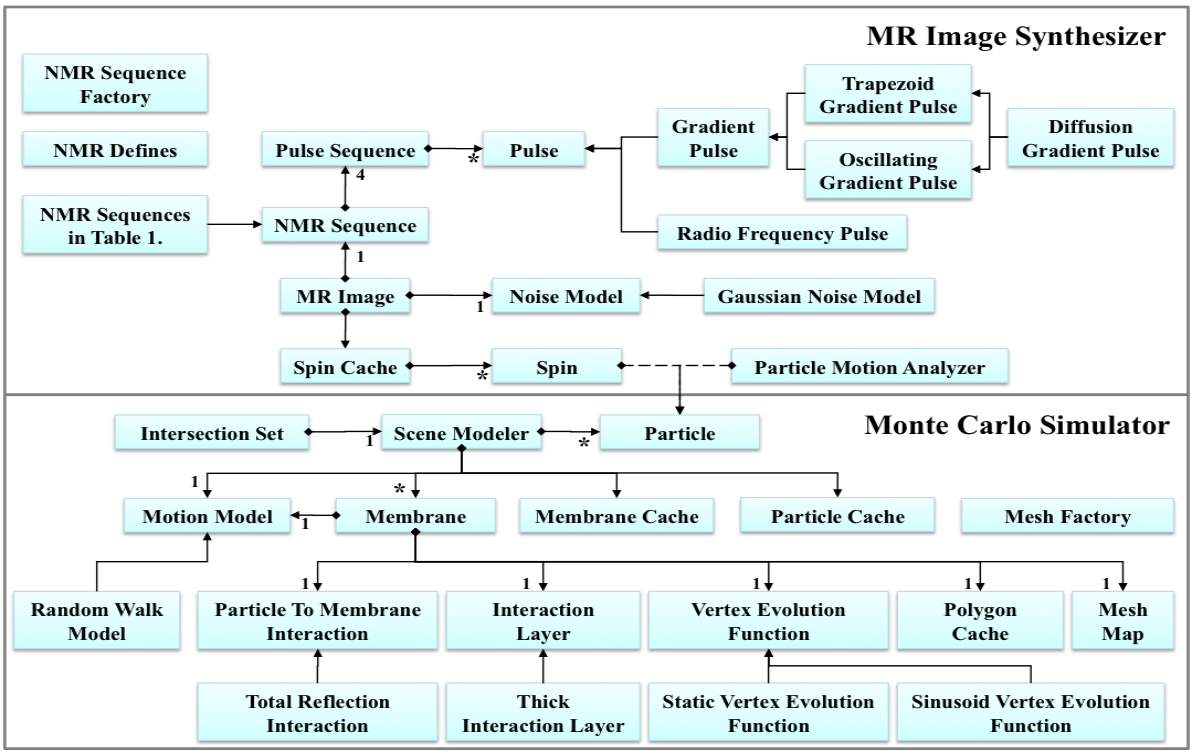

Figure 2: UML diagram of the BrainVISA/Microscopist-1.0 toolbox

Figure 3 gives a snapshot of the graphic user interface implemented for BrainVISA/Microscopist-1.0. The GUI is comprised of a control panel on the left and a visualization window on the right that allows to visualize the membrane scene mimicking a biological tissue of interest, a sub-sampling of the particle set with dynamic rendering, and the trajectories of these particles.

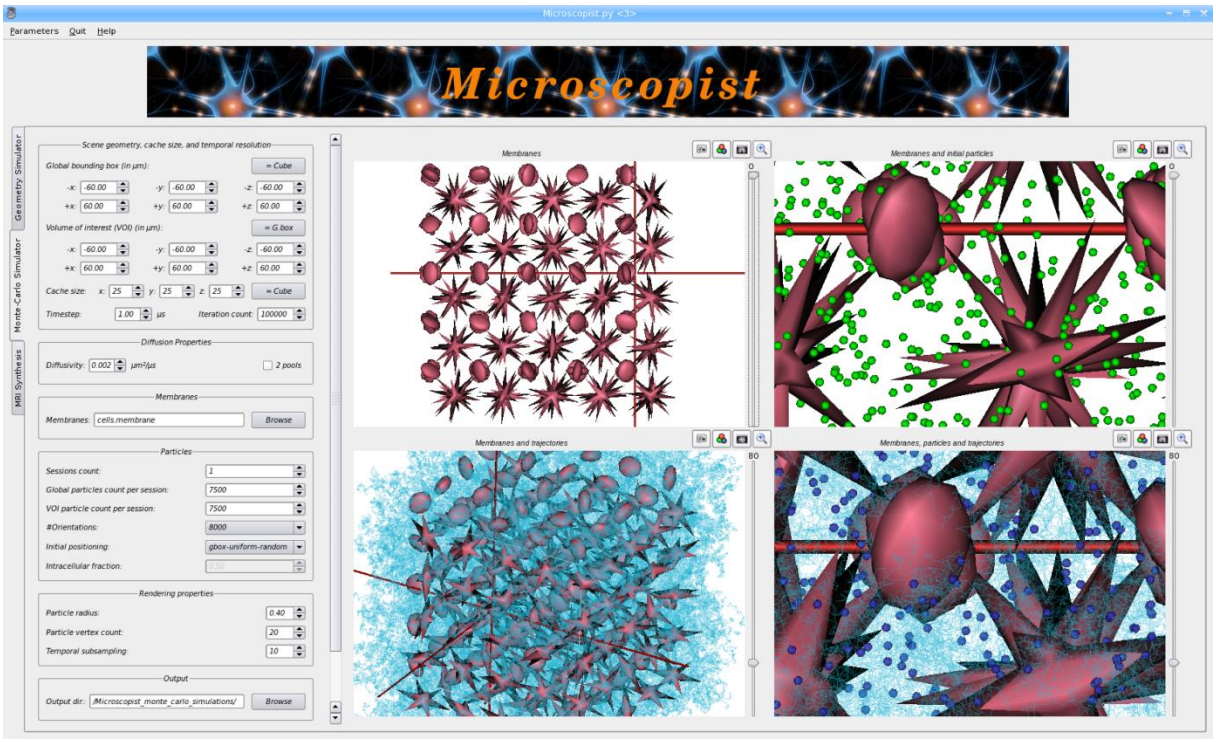

Figure 3: graphic user interface of BrainVISA/Microscopist-1.0

IN SILICO EXPERIMENTS FOR VALIDATION

In order to validate the BrainVISA/Microscopist toolbox, several experiments have been conducted on synthetic membrane environment assuming simple modelling of the diffusion process.

Several in silico experiments were conducted to check the accuracy and robustness of BrainVISA/Microscopist to simulate geometrical configurations of brain tissue environments and extract information about their microstructure:

- **multiple scattering experiment**: we utilized DMS to create a simulation space (460x400x1,000 μm^3) where straight parallel impermeable cylinders with 1,000 µm in length were placed on a 24x24 hexagonal lattice with a center spacing of 19.1 um. WM fibers were modeled using impermeable cylindrical membranes with a diameter of 19 um were built by meshes using 40 polygons per cylinder. We performed the random walk MC simulation using N_p = 5x10^5, N_l = 10^5, and t_s = 5 us. The compartmental D of 0.002 mm^2/s was assumed to be identical in the intra- and extra-cellular spaces. Synthetic DW datasets were then collected using single and double PGSE sequences with □/□/T_M = 2/200/0 ms. A range of G (S_R = 5,000 T/m/s) from 0 to 1,200 mT/m with a 10 mT/m increment were applied for the single PGSE, and 0 to 6,00 mT/m with a 5 mT/m were used for the double PGSE. The DW gradient was applied in a perpendicular direction to the fibre axis. Figure 4 showed the results of echo DW signal attenuation obtained from the single and double PGSE measurements. For comparison, the signal decay was plotted against 2q for the double PGSE. The first diffusion-diffraction trough was observed at a q-value of 655.7 cm^{-1} for both sequences, corresponding to an estimated fibre diameter of 18.6 (= 1.22x10^4 / 655.7) um

based on Callaghan theory (Callaghan, 1993).

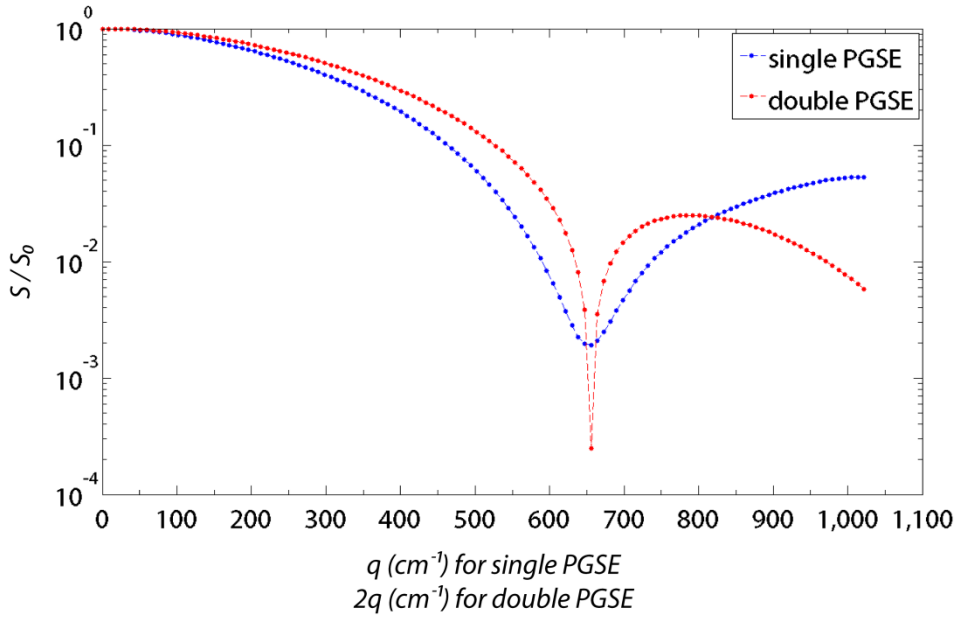

Figure 4 - Diffusion-diffraction patterns obtained from single and double PGSE experiments. The diffraction trough occurred at q = 655.7 cm^{-1}, giving an estimated compartment size (i.e. fibre diameter) of 18.6 μm. The result was closed to the actual diameter of 19 μm used in the MC simulations.

- **temporal diffusion spectroscopy experiment**: We followed the simulations proposed by Xu et al. (Xu et al., 2009) and then extended using different oscillation waveforms and frequencies. We generated a simulation space (50×50×200 μm^3) where straight parallel cylinders with 200 μm in length were placed on a 25×25 cubic lattice with the center spacing of 2.1 μm. Impermeable cell membranes with a diameter of 1.96 μm similar to the axon size of human brain were built by meshes using 40 polygons. The size of the spatial subvolume was 25×25×100. We performed the random walk MC simulation using N_p = 10^6, N_l = 72,000, and t_s = 1 μs. The compartmental D of 0.002 mm^2/s was assumed to be identical in the intra- and extra-cellular space. Synthetic DW datasets were then collected using cosine-, sine-, and double-sine-modulated OGSE diffusion sequences (Does et al., 2003) with a fixed waveform duration of 20 ms, which resulted in a TE of 50.5 ms. For each gradient waveform, seven oscillating frequencies (f = 0.1/0.2/0.4/0.8/1.2/1.6/2.0 kHz) were used to study the frequency dependency, giving a range of effective diffusion times (Δ_e) from 37.5 to 0.125 ms. For each f, the transverse DW signal was calculated at 11 b-values ranging from 0 to 500 s/mm^2 obtained by varying the gradient amplitude G. Figure 5 showed the DW signal attenuation and its dependence on the oscillating waveform and frequency. For each waveform, larger signal decay was observed at a higher frequency of DW gradients, i.e. the apparent diffusion coefficient was higher at a short effective diffusion time. The results were consistent with those shown by Does et al. (Does et al., 2003) and Xu et al (Xu et al., 2009).

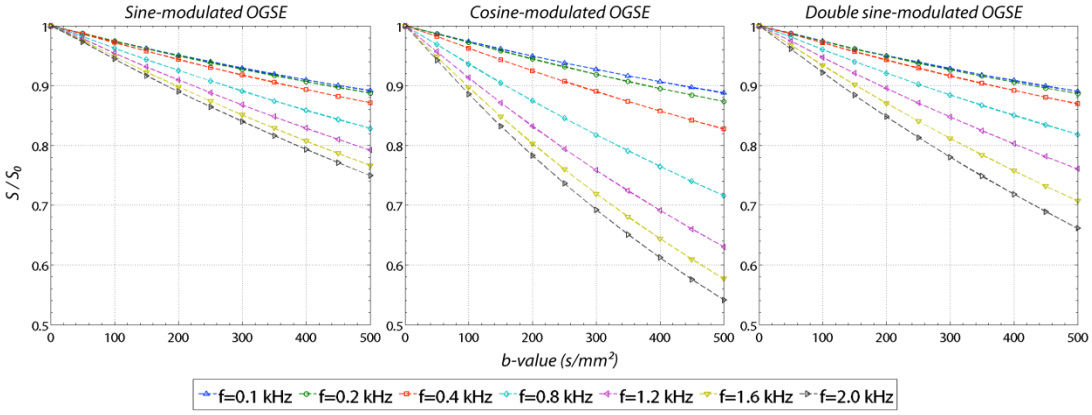

Figure 5 - Simulated DW signal attenuation obtained from the modeled WM tissue using a cosine-modulated (left), sine-modulated (middle), and a double-sine-modulated OGSE sequences (right).

- **fiber-tracking experiment**: In the last experiment, we demonstrate the application on high angular resolution diffusion imaging (HARDI) and fibre tractography. DMS was utilized to simulate three WM fibre configurations, namely crossing, kissing, and branching fibres, in separate simulation spaces with dimensions of 110×190×150, 110×190×150, and 200×210×185 μm^3, respectively (see Figure 6). Each fibre had a diameter of 5 μm and no permeability. The parameters for the MC simulations were: $N_p = 10^6$, N_l = 8,000, t_s = 10 μs, and D = 0.002 mm^2/s. We utilized a conventional single-PGSE pulse sequence to synthesize HARDI data with the following sequence parameters: G = 40 mT/m, S_R = 200 T/m/s, δ/Δ/TE = 34.75/40.75/80 ms, and b-value = 4,000 s/mm^2. For each fibre configuration, DW images were synthesized using a grid volume that produced a single slice image with an inplane resolution of 5×5 μm^2. A uniform HARDI sampling scheme consisted of 200 unique orientations created by an electrostatic repulsion model (Jones et al., 1999b). For each fibre configuration, we reconstructed the fibre orientation distribution function (fODF) using the sharpening deconvolution transform (SDT) with a spherical harmonic order of 6 (Descoteaux et al., 2009). In addition, DT analysis was performed to obtain the fractional anisotropy (FA) map, which was utilized to create mask images for fibre tracking. Both deterministic and probabilistic fibre tractography were obtained via a streamline fibre-tracking algorithm, with a forward step increment of 1.25 μm, an aperture angle of 30º (Basser et al., 2000; Descoteaux et al., 2009). Figure 7 showed the results of fODF and probabilistic tractography for crossing and kissing fibre tracts. SDT gave different fODF patterns in the crossing and kissing fibres, and the streamline probabilistic fibre tractography generated based on SDF-fODF can successfully differentiate fibres pathways. Figure 8 illustrated the results of fibre tracking using deterministic and probabilistic methods. The deterministic fibre tractography resulted in ambiguous fibre tracts in the region where the fibre tracts diverted into two different directions. The probabilistic fibre tractography showed better correspondence with the simulated fibre configuration (i.e. the ground truth).

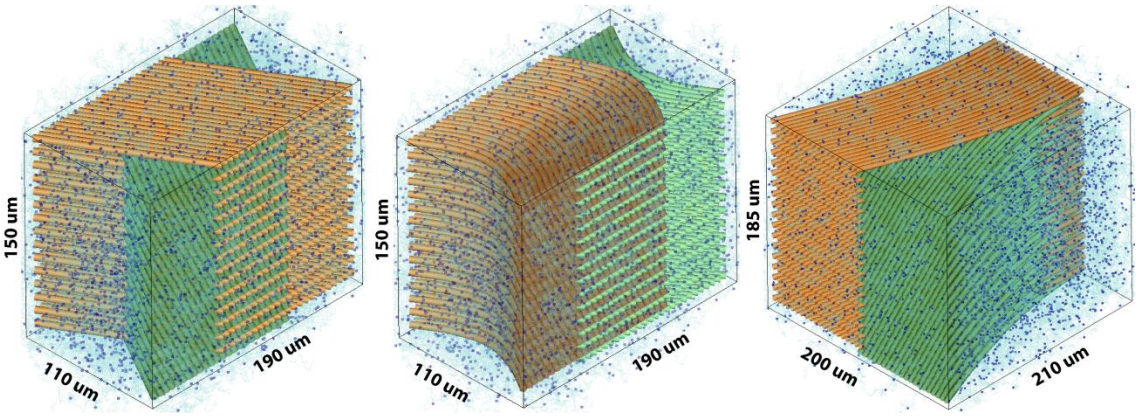

Figure 6 - DMS was utilized to create three fibre configurations typically observed in human brains. Left column: crossing fibres; middle column: kissing fibres; right column: branching fibres. For each case, two networks of fibres, coloured in green and orange, were arranged in an interleaved fashion. A subset of diffusing particles and their motion trajectories were illustrated by dark blue spheres and light blue curves.

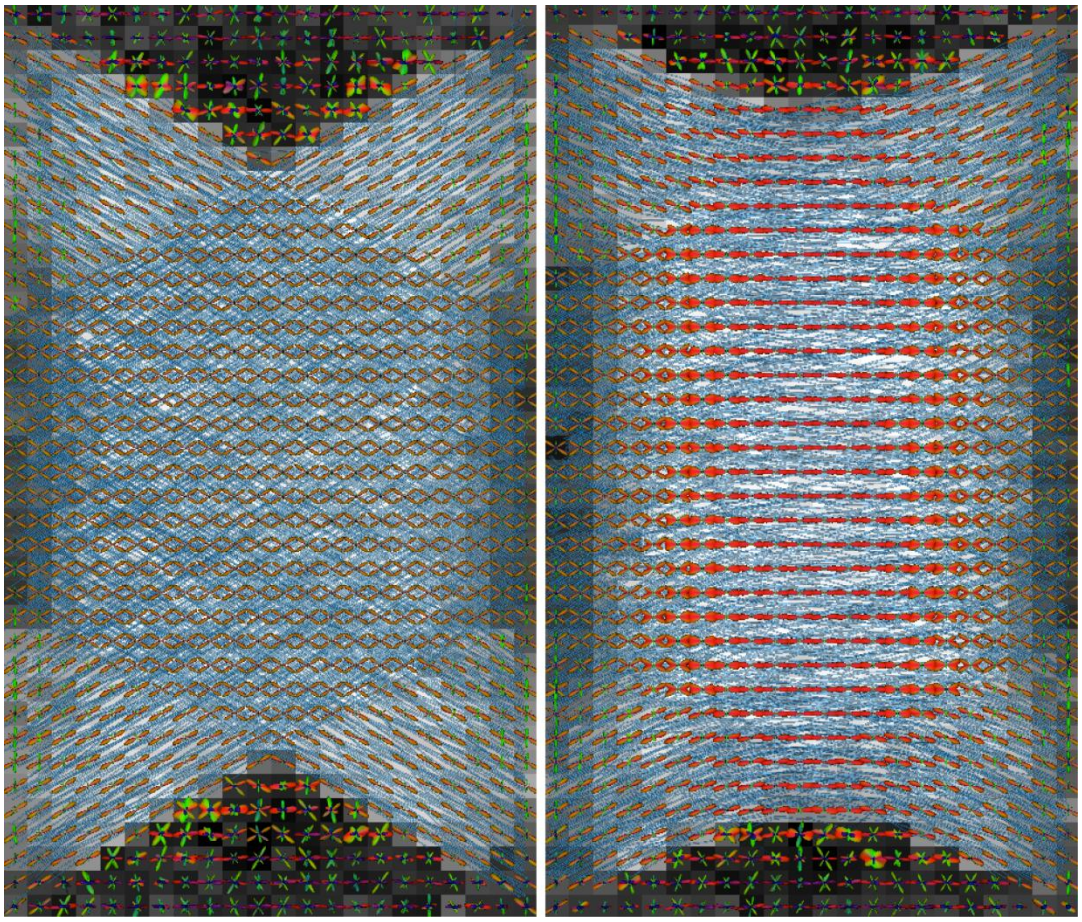

Figure 7 - The sharpening deconvolution transform and the streamline probabilistic fibre-tracking algorithm were performed on the synthetic DW datasets of crossing (left) and kissing (right) fibres. The fODF were color-coded depending on orientations (red: left-right, green: top-down, blue: inferior-superior). Fibre tractography was represented by cylinders colored in blue. Both of the fODF and tractography were overlapped on the FA images.

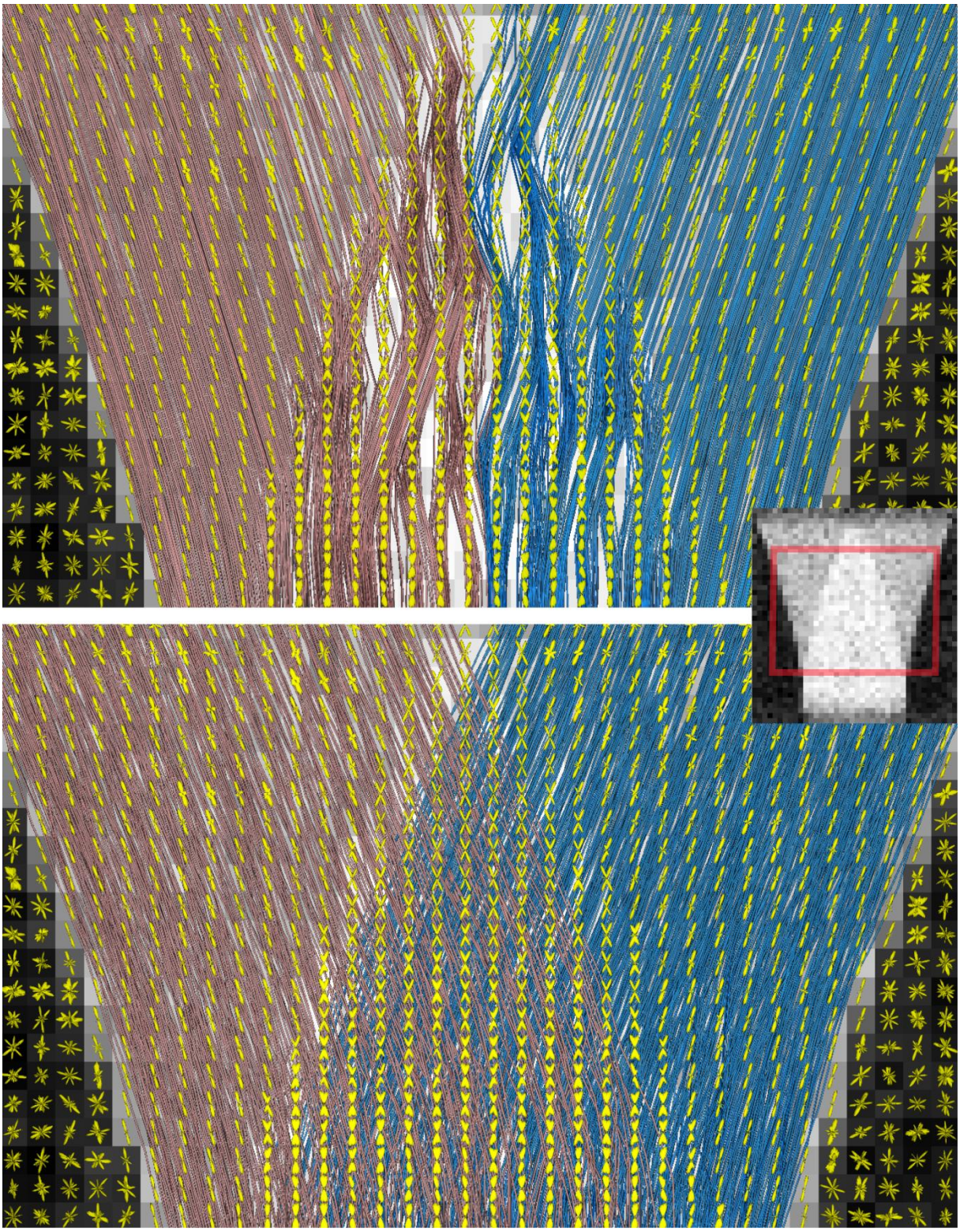

Figure 8 - Top row: fibre tracking using a deterministic approach. Bottom row: fibre tracking using a probabilistic approach. fODF were colored in yellow. Center: the location of fibre tractography on FA map.

Bibliography:

- Basser, P.J., Pajevic, S., Pierpaoli, C., Duda, J., Aldroubi, A., 2000. In vivo fiber tractography using DT-MRI data. Magn Reson Med 44, 625-632.
- Callaghan, P.T., 1993. Principles of nuclear magnetic resonance microscopy, 1 ed. Oxford University Press, USA.
- Descoteaux, M., Deriche, R., Knösche, T.R., Anwander, A., 2009. Deterministic and probabilistic tractography based on complex fibre orientation distributions. IEEE Trans Med Imaging 28, 269-286.
- Does, M.D., Parsons, E.C., Gore, J.C., 2003. Oscillating gradient measurements of water diffusion in normal and globally ischemic rat brain. Magn Reson Med 49, 206-215.
- Jones, D.K., Horsfield, M.A., Simmons, A., 1999a. Optimal strategies for measuring diffusion in anisotropic systems by magnetic resonance imaging. Magn Reson Med 42, 515-525.
- Xu, J., Does, M.D., Gore, J.C., 2009. Quantitative characterization of tissue microstructure with temporal diffusion spectroscopy. J Magn Reson 200, 189-197.

IN SILICO EXPERIMENTS TO INFER THE TISSUE CYTOARCHITECTURE AND ITS DYNAMICS DURING BRAIN ACTIVATION

Using the BrainVISA/Microscopist toolbox, we addressed two scientific questions of interest:

- how does the cell swelling impact the apparent diffusion coefficient during brain activation?
- Can we robustly probe the axon radii using clinical MRI systems ?

Study of the impact of cell swelling on the apparent diffusion coefficient

Diffusion-weighted (DW) MRI has been extensively applied to clinical diagnosis and brain research. In the literature, cell swelling has been proposed to be a major factor responsible for the variation of apparent diffusion coefficient (ADC) in acute ischemic stroke and neuronal activation, whereas the detailed mechanism requires further clarification. Thus, we investigated the influence of dynamic changes in cell size on ADC using BrainVISA/Microscopist. To our knowledge, this is the first study to represent the active cell swelling in a three-dimensional DW-MRI simulation.
Monte Carlo simulations were performed to simulate water diffusion in a network of spherical neural cells. Their surfaces were built using meshes and incorporated with an evolution function to simulate morphological variations. First, we used a static function to run nine simulations, where the cell size was fixed at 9.0-9.8 µm respectively. Second, we utilized a sinusoid function (amplitude=0.2µm) to simulate cell swelling in four simulations, where the initial cell sizes were 9.0/9.2/9.4/9.6 µm. Each simulation employed 10^6 particles and 5500 iterations.
Synthetic DW signals were acquired from a simulated pulsed-gradient spin echo sequence using a *q*-space sampling scheme comprising 60 directions at a *b*-value of 1000 s/mm^2.
ADC was estimated using a diffusion tensor analysis on synthetic DW dataset and determined by averaging the eigenvalues of the tensor model.
Fig. 9 illustrates the Monte Carlo simulation environment and the obtained apparent diffusion coefficint. A reduction of ADC was observed while the cell size increased for both static and dynamic size variations. For the case of dynamic cell swelling, we found that the ADCs were closed to the mean value of their extrema radii.
We verify that cell swelling results in a drop of ADC, which is consistent with the clinical findings on acute ischemic stroke published by Moseley in the 90's. Moreover, importantly, we show that the dynamic cell-membrane expansion also results in a decrease in ADC; therefore the cell swelling induced by neuronal activation is partly responsible for the reduced diffusivity in a functional DW-MRI experiment.

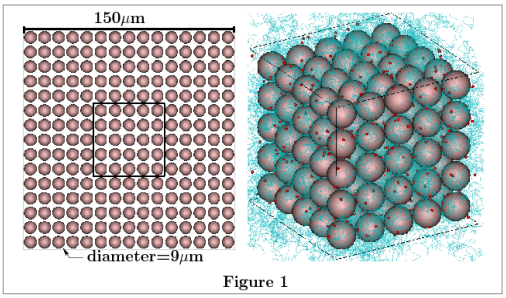

Figure 1

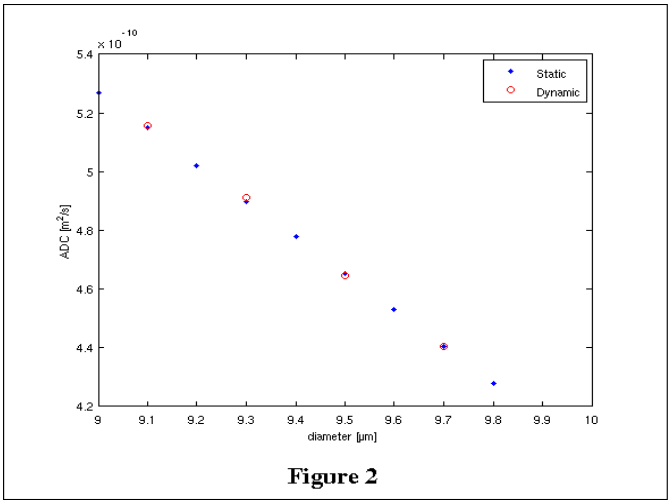

Figure 2

Figure 9: effect of cells swelling on the apparent diffusion coefficient; a reduction of the ADC was observed while the cell size increased for both static and dynamic size variations

Robust estimation of axon radii using clinical MRI systems

The advanced diffusion-weighted (DW) MR microscopy imaging has been proved to be efficient to probe microstructural features of tissues, such as cell size, fiber density, and membrane permeability [1-3]. These direct measures of tissue properties can be utilized as biomarkers to monitor tissue status. Although a number of elaborate imaging protocols have been proposed for microstructures imaging, such us multiple pulsed-gradient spin echo (PGSE) and oscillating gradient approaches, the conventional PGSE sequence remains the most commonly used especially on clinical MR scanners due to its capability of the gradient system. The method is able to effectively optimize the DW MR imaging protocol for measuring the fiber/cellular sizes found in the human brains, whereas the difficulties for clinical studies remain in two aspects. Firstly, the optimized imaging strategy is generated for a specific fiber radius whereas the white matter (WM) of human brain covers a range of fiber radii approximately from 1 to 10 um; secondly, a high gradient intensity (~200 mT/m) is required for accurate estimation of small fiber radius, which is less applicable to clinical MR scanners where the maximum gradient amplitude is limited to 40 mT/m. Accordingly, in this study, we used a Monte Carlo simulator to simulate water diffusion in various fiber radii, and then evaluate a list of PGSE imaging protocols under the constraint on the gradient system capability of clinical MR scanners.

Simulations were performed using a random walk Monte Carlo simulator to simulate 3D water molecular diffusion in a bundle of parallel impermeable fibers formed by mesh-based cylinders. We created four simulation scenes with the same the intracellular fraction (f_{IC}=0.74), where each contains specific fiber radius R (=1/2/4/6/ μm). In each simulation scene, 10^5 diffusing particles were randomly distributed, and a constant diffusivity of 2×10^{-3} mm^2/s was assumed to be identical in the intra- and extra-cellular space. We used a total iteration count of 10^4 and a simulation time step of 10 μs, yielding a step size of 0.32 μm.

Synthetic MR dataset was obtained using a PGSE sequence with trapezoidal DW gradient pulses. Table 1 summarized the list of imaging protocols created to conform to the capability of clinical MR system. Each protocol contains 120 DW acquisitions with different M and N combinations, where M is the number of q-space sampling shells and N is the number of DW gradient orientations per shell (M). In each protocol, the gradient amplitude (G) and slew rate were fixed at 40 mT/m and 200 T/m/s respectively; while the DW gradient pulse duration (δ) and separation (Δ) were varied simultaneously to keep a constant effective diffusion time ($\Delta_{eff} = \Delta - \delta/3$ = 50 ms) so as to reach sufficient diffusion sensitizing factors (i.e. b-values) for the short δs. The echo time (TE) determined by the maximum δ and Δ was fixed in each protocol, and a T2 of 70 ms typically found in WM at 3T was used.

Parameter estimation was performed using the Markov Chain Monte Carlo (MCMC) method implemented with a Rician noise model to sample the posterior distribution of model parameters [1-2]. Initial estimates

for the intracellular fraction (f_{IC}), axial and transverse diffusivities were obtained from the diffusion tensor (DT) analysis. Fiber direction (along z-axis) and radius (R) were initialized to the ground-truth values given in the Monte Carlo simulations. Synthetic Rician noise was added to the DW signal considering the effect of varying TE. The signal-to-noise ratio is 50 at TE = 86.5 ms. In the procedure of MCMC, the burn-in period, sampling interval, and sampling count were 10^5, 10^3, and 10^2 respectively.

Figure 10 shows the histograms of R estimates obtained from the posterior distribution for each true radius R, and Table 2 summarizes the standard deviation (σ) of the distributions for each case. All of the protocols can accurately estimate large radii (R = 4 and 6 μm) but produced bias for the smaller radii, especially for R = 1 μm; nevertheless, it could be still recognized as a small radius. For M = 3 (i.e. *Protocol 1-3*), both *Protocol 2&3* resulted in better R estimation than *Protocol 1*, indicating that moderate to high *b*-values were important for accurate R mapping. The similar results were found when M = 4: *Protocol 5&6* utilized higher *b*-values and resulted in shaper distributions, i.e. lower σ. For M = 5 or 6, all protocols showed good R estimation, due to the coverage of a wide range of *b*-values. *Protocol 3* (M = 3), *6* (M = 4), and *8* (M = 5) resulted in less overlapping between R = 1 and 2, and produced sharper distribution for larger radii.

We assessed the feasibility of mapping the fiber radius under the constraints of clinical MR systems. Meanwhile, we provided a guideline for the selection of experimental parameters to setup clinical protocols for the purpose of fiber radius estimation.

Table 1. Clinical PGSE DW MR imaging protocols

Protocol	M	N	δ (ms)	TE (ms)	*b*-value (s/mm^2)
1	3	40	4, 8, 12	70.5	80, 350, 800
2			8, 16, 20	81.2	350, 1430, 2250
3			16, 20, 24	86.5	1430, 2250, 3250
4	4	30	4, 8, 12, 16	75.8	80, 350, 800, 1430
5			8, 12, 16, 20	81.2	350, 800, 1430, 2250
6			12, 16, 20, 24	86.5	800, 1430, 2250, 3250
7	5	24	4, 8, 12,16, 20	81.2	80, 350, 800, 1430, 2250
8			8, 12,16, 20, 24	86.5	350, 800, 1430, 2250, 3250
9	6	20	4, 8, 12,16, 20, 24	86.5	80, 350, 800, 1430, 2250, 3250

Table 2. Mean ± Standard deviations (σ) of the distributions

Protocol	*R*=1 μm	*R*=2 μm	*R*=4 μm	*R*=6 μm
1	1.54 ± 0.68	2.11 ± 0.61	4.11 ± 0.68	5.70 ± 0.65
2	1.22 ± 0.44	1.78 ± 0.33	3.91 ± 0.29	6.07 ± 0.58
3	1.02 ± 0.31	1.86 ± 0.26	3.88 ± 0.33	5.91 ± 0.34
4	1.07 ± 0.50	1.93 ± 0.65	3.81 ± 0.50	6.11 ± 0.41
5	1.17 ± 0.31	1.84 ± 0.53	3.93 ± 0.48	6.11 ± 0.54
6	1.04 ± 0.27	1.78 ± 0.30	3.90 ± 0.38	6.12 ± 0.44
7	1.29 ± 0.35	1.95 ± 0.63	3.92 ± 0.44	6.22 ± 0.43
8	0.96 ± 0.32	1.79 ± 0.26	3.92 ± 0.27	5.94 ± 0.41
9	1.14 ± 0.37	1.69 ± 0.47	3.91± 0.35	6.00 ± 0.37

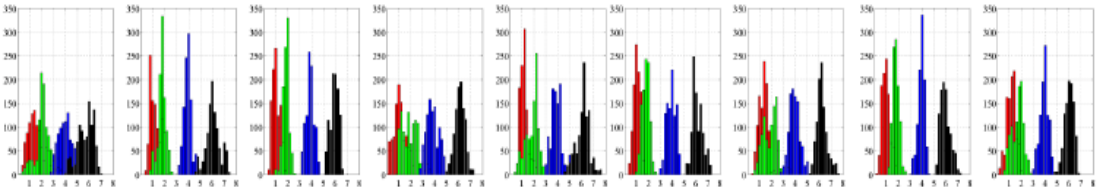

Figure 10: assessment of the use of clinical MRI systems to probe axon radii using pulsed-gradient spin echo sequences; table 1 describe the various multiple shell protocols tested with different diffusion times and b-values and the bottom of the figure provides the distributions of radii obtained for each protocol and each radius.

FUTURE EXPERIMENTS

In the frame of this grant, we have developed the required modeling and simulation tools to disentangle the encoding of the cytoarchitecture of brain tissue naturally encoded in the diffusion-weighted MRI signal. This tool reveals to be really useful to address studies aiming at modeling the diffusion MRI signal and to validate its robustness and accuracy.

We have launched an ancillar study to obtain acquisitions of brain samples using electron microscopy in order to extract more realistic membrane geometries in order to perform large simulations and to couple these simulations with high resolution MRI acquisitions that will be performed on the 17T MRI system of NeuroSpin. This work is undergoing and will certainly contribute to better understand the cytoarchitecture of the human brain.

PUBLICATIONS

Journal papers :

- Yeh CH, Le Bihan D., Li J.-R., Mangin J.-F., Lin C.-P., Poupon C., Monte-Carlo simulation software dedicated to diffusion-weighted MR experiments in neural media. (Submitted to NeuroImage)
- Yeh CH, Kezele I., Schmitt B., Li J.-R., Le Bihan D., Lin C.-P., Poupon C., Evaluation of fiber radius mapping using diffusion MRI under clinical system constraints. (Submitted to Magnetic Resonance Imaging)

Conferences :

- Yeh CH, Tournier J.-D., Cho K.-H., Poupon C., Lin C.-P., Evaluation of angular uncertainties of q-space diffusion MRI under finite gradient pulse widths : a phantom study. Proc ISMRM 2009, p. 3550.
- Yeh CH, Le Bihan D, Li JR, Mangin JF, Lin CP, Poupon C. Monte-Carlo simulation software dedicated to diffusion weighted MR experiments in neural media. In proceedings 16th HBM, 2010 (Barcelone, Espagne
- Yeh CH, Le Bihan D, Li JR, Mangin JF, Lin CP, Poupon C. Monte-Carlo simulation software dedicated to diffusion weighted MR experiments in neural media. In Proceedings ISMRM 2010 (Stockholm, Suede), abstract number 5762.
- Yeh CH, Kezele I, Alexander D, Schmitt B, Li JR, Le Bihan D, Lin CP, Poupon C. Evaluation of fiber radius mapping using diffusion MRI under clinical system constraints". In 19th ISMRM, Montreal, Canada, 2011, abstract number 2017